NASA CONTRACTOR REPORT

NASA CR-129021

STATISTICAL ANALYSIS OF FLIGHT TIMES FOR SPACE SHUTTLE FERRY FLIGHTS

By M. E. Graves and M. Perlmutter
Northrop Services, Inc.
6025 Technology Dr.
Huntsville, Alabama 35805

January 1974

Prepared for

NASA-GEORGE C. MARSHALL SPACE FLIGHT CENTER
Marshall Space Flight Center, Alabama 35812

TECHNICAL REPORT STANDARD TITLE PAGE

1. REPORT NO. NASA CR-129021	2. GOVERNMENT ACCESSION NO.	3. RECIPIENT'S CATALOG NO.
4. TITLE AND SUBTITLE STATISTICAL ANALYSIS OF FLIGHT TIMES FOR SPACE SHUTTLE FERRY FLIGHTS		5. REPORT DATE January 1974 6. PERFORMING ORGANIZATION CODE
7. AUTHOR(S) M. E. Graves and M. Perlmutter		8. PERFORMING ORGANIZATION REPORT #
9. PERFORMING ORGANIZATION NAME AND ADDRESS Northrop Services, Inc. 6025 Technology Drive Huntsville, AL 35805		10. WORK UNIT NO. 11. CONTRACT OR GRANT NO. NAS 8-21810
12. SPONSORING AGENCY NAME AND ADDRESS National Aeronautics and Space Administration Washington, D. C. 20546		13. TYPE OF REPORT & PERIOD COVERED TOPICAL CONTRACTOR 14. SPONSORING AGENCY CODE

15. SUPPLEMENTARY NOTES

Prepared under the technical direction of the Aerospace Environment Division, Aero-Astrodynamics Laboratory, Marshall Space Flight Center; contract monitor is Mr. S. C. Brown.

16. ABSTRACT

Markov chain and Monte Carlo analysis techniques are applied to the simulated Space Shuttle Orbiter Ferry flights to obtain statistical distributions of flight time duration between Edwards Air Force Base and Kennedy Space Center. The two methods are compared, and are found to be in excellent agreement. The flights are subjected to certain operational and meteorological requirements, or constraints, which cause eastbound and westbound trips to yield different results. Persistence of events theory is applied to the occurrence of inclement conditions to find their effect upon the statistical flight time distribution. In a sensitivity test, some of the constraints are varied to observe the corresponding changes in the results.

Subsequent to completion of this report NASA terminated all activities relating to the Air Breathing Engine System for the Space Shuttle Orbiter. This changed the primary mode of Orbiter ferry and flight testing to be by carrier aircraft (C5A or B747). While the change in the Orbiter ferry operation may negate the results the still-valid analysis techniques warrant publication of the report.

17. KEY WORDS	18. DISTRIBUTION STATEMENT Unclassified - unlimited Ludie G. Richard Acting Director, Aero-Astrodynamics Laboratory

19. SECURITY CLASSIF. (of this report)	20. SECURITY CLASSIF. (of this page)	21. NO. OF PAGES	22. PRICE
Unclassified	Unclassified	39	NTIS

MSFC - Form 3292 (Rev December 1972)

For sale by National Technical Information Service, Springfield, Virginia 22151

FOREWORD

The work described in this report was conducted by Northrop Services, Inc., Huntsville, Alabama, for the National Aeronautics and Space Administration, George C. Marshall Space Flight Center, Aero-Astrodynamics Laboratory, under Contract No. NAS8-21810, Appendix A, Schedule Order Numbers 13 and 14. Dr. George H. Fichtl and Mr. S. Clark Brown were the Technical Coordinators for this task.

ACKNOWLEDGEMENTS

The authors are indebted to Mr. S. Clark Brown and Mr. Kelly Hill of NASA for the use of meteorological data records and charts. They wish to thank Mr. Brown and Dr. George Fichtl of NASA for their guidance and assistance throughout the project.

PRECEDING PAGE BLANK NOT FILMED

TABLE OF CONTENTS

Section I

INTRODUCTION

Prior to the launching of a Space Shuttle Orbiter vehicle, a ferrying operation across the southern states may be carried out to move the Orbiter from assembly site to launch point or from landing point to assembly site. The proposed route of this operation (Figure 1) has seven terminals and a like number of alternates for route segments averaging about 350 miles. The terminals are subject to certain landing and takeoff constraints and the route segments are subject to altitude and headwind constraints. The objective of this study is to find the distribution in time of flight duration between Edwards AFB and Kennedy Spaceflight Center (KSC) under these constraints, using meteorological data for the four midseasonal months of January, April, July, and October.

To determine this distribution, two distinct statistical techniques have been used. The first is a Markov chain process and the second is a Monte Carlo method. A certain ferry configuration, a vehicle cruising speed of 250 knots, and some environmental constraints have been set for this particular problem. However, the two statistical methods are entirely applicable to other ferry configurations and other operational values of the variables pertaining to speed limitations and environmental requirements.

To the best of the authors' knowledge, there is no previous work which is directly applicable to this topic. However, the Markov chain theory has been used by Brodie [1] in solving the similar problem of finding the probability of success of a space mission. A large amount of work has been done on model simulation with the Monte Carlo method (e.g., Schreider [2]).

The study is divided into seven sections. The Markov chain theory is presented in Section II, with application to the simulation of Orbiter ferry flights. The flights are subject to certain persistence effects, so the Markov procedure is outlined for meteorological data which contain persistence as well as for data which are free of persistence.

Section III presents an adaptation of the Monte Carlo theory to the problem at hand, again treating the procedure for data containing persistence effects separately from persistence-free data.

Section IV deals with the transition probabilities of Markov chain theory. After discussing the theoretical aspects of this topic, the application to ferry simulation is made by quantifying the Shuttle Orbiter ferry requirements. These constraints are related to hydrometeors, ceiling, visibility, inflight headwinds, and runway density. The effects of persistence in cruise headwinds and in hydrometeors, or inclement weather, are also evaluated.

Section V presents a number of distributions of flight duration under various assumptions, using both the Markov chain and Monte Carlo procedures. The degree of sensitivity of the results to changes in the cruise headwinds requirements and ceiling/visibility constraints is also tested, and the outcome when there is mutual dependence among the hydrometeors and the ceiling/visibility constraint is investigated to give an optimistic, limiting assessment.

Finally, the conclusions of this investigation are presented in Section VI, the references are shown in Section VII.

Section II

MARKOV CHAIN THEORY

Two applications of Markov Chain theory will be considered. The first case excludes the persistence of unfavorable conditions. The second case includes such effects. The two cases are presented in subsections 2.1 and 2.2, respectively. In subsection 2.3, the effect of additional independent delays is investigated.

2.1 MARKOV THEORY WITHOUT PERSISTENCE EFFECTS

Markov theory deals with processes in which the probability of obtaining a particular state in the n^{th} trial depends only upon the state preceding the trial. To illustrate, the probability of obtaining a chain of events E_o, E_1, ... E_n can be written as $P(E_o, E_1, \ldots E_n) = P(E_o)\, P(E_1/E_o) \ldots P(E_n/E_{n-1})$. Here $P(E_o)$ is the probability of being in the initial state E_o. $P(E_1/E_o)$ is the conditional probability of passing from state E_o to E_1 in the first trial.

In the simplest Shuttle ferrying case, the possible states can be assumed to be

$$E = \begin{bmatrix} a_1 \\ a_2 \\ \cdot \\ \cdot \\ \cdot \\ a_7 \end{bmatrix} = [a_i],\ i = 1, 2, \ldots, 7 \qquad (1)$$

where a_1 is the initial airport, a_2 is the terminal for the first leg, etc. (see Figure 1), and a_7 is the final destination. Taking initially the case where all flights begin at the same airport, then $P(E_o)$ becomes

$$P(E_o) = \begin{bmatrix} P(a_1) \\ P(a_2) \\ \cdot \\ \cdot \\ \cdot \\ P(a_7) \end{bmatrix} = \begin{bmatrix} 1 \\ 0 \\ \cdot \\ \cdot \\ \cdot \\ 0 \end{bmatrix} = [I_i],\ i = 1, 2, \ldots 7 \qquad (2)$$

where $[I_i]$ is equivalent to $P(E_o)$.

The term $P(E_n/E_{n-1})$ is the conditional probability of going from state E_{n-1} to state E_n in the n^{th} trial. This can be written as the matrix of transition probabilities,

$$P(E_n/E_{n-1}) = \begin{bmatrix} T_{1,1} & T_{1,2} & 0 & 0 & 0 & 0 & 0 \\ 0 & T_{2,2} & T_{2,3} & 0 & 0 & 0 & 0 \\ 0 & 0 & T_{3,3} & T_{3,4} & 0 & 0 & 0 \\ 0 & 0 & 0 & T_{4,4} & T_{4,5} & 0 & 0 \\ 0 & 0 & 0 & 0 & T_{5,5} & T_{5,6} & 0 \\ 0 & 0 & 0 & 0 & 0 & T_{6,6} & T_{6,7} \\ 0 & 0 & 0 & 0 & 0 & 0 & 1 \end{bmatrix} \qquad (3)$$

$$= [T_{i,j}],\ i = 1, 2, \ldots, 7,\ j = 1, 2, \ldots, 7$$

Here, $T_{7,7}$ is set equal to 1 because state a_7 is the absorbing state, or final destination. The zeroes represent the transition probabilities for nonadjacent airports; all flights operate between adjacent airports.

If persistence effects are excluded, then the states E (or a_i) refer to the airports along the route A_i (Figure 2a). Each trial is considered to require half a day. The transition probability, T_{i+1}, gives the probability of leaving airport A_i and reaching the next airport, A_{i+1}, during the half-day trial period. The transition probabilities for morning trials are different from those for afternoon trials.

In Figure 2a the initial state a_1 is shown at 1 (A.M.). This can be assumed to be N identical aircraft at the first airport ready for the first morning trial. A fraction $T_{1,2}$ of N will be successful and proceed as shown in Figure 2a to point a_2, the second airport, at 1 (P.M.), ready for the afternoon trial. The remainder $N(1-T_{1,2}) = N\ T_{1,1}$ will be unsuccessful and remain at a_1 at 1 (P.M.) ready for the afternoon trial.

After the afternoon trial, there is a probability $T_{2,3}$ of the aircraft at airport a_2 moving to airport a_3 at 2 (A.M.).

The probability of reaching state a_7, which is the final destination after a given number of trials, is the result being sought. The probability of attaining state a_7 after the first event is

$$P(1/a_7) = \sum_{i=1}^{7} I_i T_{i,7} = 0 \qquad (4a)$$

after 2 events,

$$P(2/a_7) = \sum_{i=1}^{7} I_i \left(\sum_{j=1}^{7} T_{i,j}\ T_{j,7} \right) = \sum_{i=1}^{7} I_i\ T_{i,7}^{(2)} = 0 \qquad (4b)$$

The probability of reaching the final airport after n half-days is

$$P(n/a_7) = \sum_{i=1}^{7} \sum_{j=1}^{7} \cdots \sum_{m=1}^{7} I_i\ T_{i,j}\ T_{j,k} \cdots T_{m,7} = \sum_{i=1}^{7} I_i\ T_{i,7}^{(n)} \qquad (4c)$$

where

$$T_{i,7}^{(2)} = \sum_{j=1}^{7} T_{i,j}\ T_{j,7} \qquad (5a)$$

$$T_{i,7}^{(3)} = \sum_{j=1}^{7} \sum_{k=1}^{7} T_{i,j}\ T_{j,k}\ T_{k,7} \qquad (5b)$$

$$T_{i,7}^{(n)} = \sum_{j=1}^{7} \cdots \sum_{m=1}^{7} T_{i,j}\ T_{j,k} \cdots T_{m,7} \qquad (5c)$$

Since all aircraft are at the first airport initially, Eqs. (5) becomes

$$P(n/a_7) = \sum_{j=1}^{7} \cdots \sum_{n=1}^{7} (1)T_{1,j}\ T_{j,k} \cdots T_{n,7} = T_{1,7}^{(n)} \qquad (6)$$

This matrix multiplication can be carried out directly.

$$S_t = \sum_{n=0}^{t} P(n/a_7) \qquad (7)$$

is also of interest. It gives the probability of reaching the final airport on or before the t^{th} trial.

2.2 MARKOV THEORY WITH PERSISTENCE EFFECTS

In this section, the term "persistence" signifies the effect of unfavorable conditions of the previous trial on the transition probabilities of the next trial. Such conditions signify that the previous trial was a "No go" outcome. Persistence is taken into account by redefining the Markov states as

$$E = \begin{bmatrix} a_1 \\ a_2 \\ \cdot \\ \cdot \\ \cdot \\ a_m \end{bmatrix} \tag{8}$$

where a_1 now refers to being located at the initial airport under previously favorable conditions; $A_1(F)$ a_2 now refers to being located at the initial airport under previously unfavorable conditions: $A_1(U)$ a_3 refers to being located at the next airport with previous conditions favorable; A_2 (F) a_4 is similar to a_3 but with previous conditions unfavorable, A_2 (U) and so forth. Then as in Eq. (2), taking initially the cases where all flights begin at the same initial airport, $P(E_o)$ is redefined as

$$P(E_o) = \begin{bmatrix} P(a_1) \\ P(a_2) \\ P(a_3) \\ P(a_4) \\ \cdot \\ \cdot \\ \cdot \\ P(a_{13}) \end{bmatrix} = \begin{bmatrix} P(F) \\ P(U) \\ 0 \\ 0 \\ \cdot \\ \cdot \\ \cdot \\ 0 \end{bmatrix} = [I_i] \tag{9}$$

where P(F) is the probability of the previous weather being favorable while P(U) is the probability of the previous weather being unfavorable.

As before, the N identical aircraft are started at airport 1. However, this time a certain fraction P(F) have previously favorable weather and are in state a_1, while the other fraction $P(U) = 1 - P(F)$ are considered to have previously unfavorable weather and are in state a_2 (Figure 2b).

The transition probability $T_{1,3}$ in Figure 2b gives the fraction of aircraft at the first airport with favorable previous weather a_1 at 1 (A.M.) that successfully reach the second airport, or state a_3, at 1 (P.M.) after the first morning trial. $T_{1,2}$ gives the other unsuccessful fraction which remain at the first airport but now with the previous weather unfavorable (e.g., state a_2) at 1 (P.M.) after the morning trial.

Similarly, the transition probability $T_{2,3}$ in Figure 2b gives the fraction of aircraft at the first airport with unfavorable previous weather state a_2 at 1 (A.M.), that successfully reaches the second airport, or state a_3 at 1 (P.M.), after the morning trial. $T_{2,2}$ gives the unsuccessful fraction which remain at the first airport in state a_2 at 1 (P.M.) after the first trial.

The probability of reaching the final destination in n trials is now given by

$$P(n/a_{13}) = \sum_{i=1}^{13} \sum_{j=1}^{13} \cdots \sum_{n=1}^{13} I_i T_{i,j} \cdots T_{n,13} = \sum_{i=1}^{13} I_i T_{i,13}^{(n)} \tag{10a}$$

The cumulative distribution is now given, as in Eq. (9), by

$$S_t = \sum_{n=0}^{t} p(n/a_{13}) \tag{10b}$$

2.3 ADDITIONAL INDEPENDENT DELAYS

During the flights, there will be occasions when an independent, additional delay beyond the previously calculated delays may occur. For instance a large scale weather formation may extend the overall flight time. The probability of an additional delay of d days of a flight can be written as p_d. Then the probability $P_d(t)$ of reaching the destination in t days can be written as

$$P_d(t) = P(t)[1 - \sum_{d=1}^{\infty} p_d] + \sum_{d=1}^{t} p_d \, P(t-d) \tag{11}$$

where P(t) is the probability of completing the trip in t days without the independent additional delay and P(t-d) is the probability of completing the trip in t-d days without such a delay.

The cumulative distribution as in Eq. 7 will now become

$$S_{d,t} = \sum_{n=0}^{t} P_d(n) \tag{12}$$

Section III

MONTE CARLO THEORY

In this section the Monte Carlo analysis is discussed. Subsection 3.1 is the case without persistence effects while subsection 3.2 extends the analysis to include the effects of persistence.

3.1 MONTE CARLO THEORY WITHOUT PERSISTENCE EFFECTS

Model sampling can be used to evaluate the probable number of days needed to reach the final destination. The simulated aircraft is started at the initial airport and its new location is calculated after the first event by the transition probability, $T_{i,j}$ where $T_{1,1} + T_{1,2} = 1$. As before, the two subscripts indicate the airports of origin and of termination, respectively. A random number which is uniformly distributed between 0 and 1 is generated. If it is less than $T_{1,2}$, the simulated aircraft is moved to the next airport. Otherwise, the aircraft is held at its present location. Its new position is calculated similarly for the next event. This process is continued until the simulated aircraft reaches the final airport after t events. It is then scored in the t-category. This process is then repeated for N samples. The probability of reaching the final destination after t trials can then be estimated by

$$P(t/a_7) \doteq n_t/N, \tag{13}$$

where n_t is the number of simulations that reach the final destination in t trials, and N is the total number of simulations.

The 95-percent confidence limits in n_t/N, δ, are given by Schreider [2] as

$$|n_t/N - P(t/a_7)| = \delta \leq 1.96 \sqrt{P(t/a_7)(1 - P(t/a_7))/N} = 1.96\ \sigma \tag{14}$$

This expression can be evaluated directly as before.

3.2 MONTE CARLO THEORY WITH PERSISTENCE EFFECTS

The Monte Carlo procedure can be modified, as was the Markov chain method, to include the effects of persistence. If P(F) is the probability of favorable conditions on a given day, the simulated aircraft is started at the initial airport by picking a random number uniformly distributed between 0 and 1 and comparing it with P(F). If the random number is less than P(F), then the previous weather is considered favorable; otherwise, it is considered unfavorable. If the previous weather is favorable, $T_{1,3}$ is used in the next trial; if not, $T_{2,3}$ is used. As discussed previously, this procedure is continued to find

$$P(t/a_{13}) \quad n_t/N \qquad (15)$$

Section IV

TRANSITION PROBABILITIES

In this section, the transition probabilities used in the analysis are discussed. In subsection 4.1, the theoretical aspects are considered, first excluding persistence and then including this factor in the discussion. In subsection 4.2, the Shuttle Orbiter Ferry requirements are quantified with persistence effects excluded. In subsection 4.3, the persistence effects are then added.

4.1 THEORETICAL ASPECTS

4.1.1 Theoretical Aspects Without Persistence

Consider a number of factors called A_1, A_2, ... A_i. If any of these events occur, the aircraft will not proceed. The probability of events A_1 or A_2 or ... or A_i occurring is given by

$$P(A_1 \text{ or } A_2 \text{ or } \dots \text{ or } A_i) = \sum_{j=1}^{i} P(A_j) - \sum_{\substack{j,k \\ j \neq k}} P(A_j A_k) + \sum_{\substack{j,k,m \\ j \neq k \neq m}} P(A_j\ A_k\ A_m) - \dots = T_{i,i} = 1 - T_{i,j} \tag{16}$$

If A_i and A_j are mutually exclusive, then

$$P(A_i A_j) = P(A_i)\ P(A_j/A_i) = 0 \tag{17a}$$

If A_i and A_j are independent events, then

$$P(A_i A_j) = P(A_i)\ P(A_j/A_i) = P(A_i)\ P(A_j) \tag{17b}$$

If A_i and A_j are inclusive, so that whenever A_i occurs A_j must occur,

$$P(A_i A_j) = P(A_j/A_i)\ P(A_i) = P(A_i) \tag{17c}$$

These relationships will be used to evaluate the overall transition probabilities for the various operational constraints.

4.1.2 Theoretical Aspects With Persistence

Consider as before a number of factors $A_1, A_2, \ldots A_K$. If any of these events occur, the trial will be unfavorable, so that

$$U_t = (A_1 \text{ or } A_2 \text{ or } \ldots)_t \tag{18}$$

The probability of unfavorable weather in the present trial, given that the previous trial was unfavorable, is

$$\begin{aligned} P(U_t/U_{t-1}) &= P[[A_1 \text{ or } A_2 \text{ or } \ldots]_t/U_{t-1}] \\ &= \sum_i P[(A_i)_t/U_{t-1}] - \sum_{\substack{j,k \\ j\neq k}} P[(A_j,A_k)_t/U_{t-1}] + \\ &\quad + \sum_{j,k,m} P(A_jA_kA_m)_t/U_{t-1}] - \ldots \\ &= T_{2,2} \text{ or } T_{4,4} \text{ or } \ldots \end{aligned} \tag{19}$$

These quantities define the persistence factors desired in the calculation.

If A_j is independent of the previous unfavorable weather, then

$$P[(A_j)_t/U_{t-1}] = P(A_j) \tag{20}$$

It can be seen that

$$P[F_t/U_{t-1}] = 1 - P[U_t/U_{t-1}] = T_{2,3} \text{ or } T_{4,5} \tag{21}$$

which is the probability of a "Go", or favorable weather on the present trial, F_t, given the previous trial was unfavorable, U_{t-1}.

As given in Reference [3],

$$P[F_t/F_{t-1}] = 1 - \frac{P[U]\ P[F_t/U_{t-1}]}{[1 - P(U)]} = T_{1,3} \text{ or } T_{3,5} \text{ or } \ldots \tag{22}$$

From this result,

$$P[U_t/F_{t-1}] = 1 - P[F_t/F_{t-1}] = T_{1,2} \text{ or } T_{3,4} \text{ or } \ldots \qquad (23)$$

4.2 QUANTIFICATION OF SHUTTLE ORBITER FERRY REQUIREMENTS

The takeoff, landing, and inflight constraints specified for this study include: (1) operation under visual flight rules with no icing; (2) acceptable ceiling and visibility at the point of origin and the destination upon landing or taking off; (3) tolerable inflight headwinds; and (4) acceptable runway atmospheric density for takeoff. The first three of these constraints are somewhat interrelated, as is indicated in the Venn diagrams for eastbound and westbound flights (Figure 3). The amount of interaction displayed in the diagrams is merely figurative. The symbols are explained in subsections 4.2.1 to 4.2.4.

To quantify the constraints, certain meteorological variables observed at the seven air bases were selected and their monthly summaries [4] were obtained over as long a period of record as possible. In general, the period of record exceeds 20 years. The meteorological variables which enter into the computation of transitional probability are listed in Table 4-1 with their specified constraining values in some cases. The effects of possible long-term weather trends were not considered because of insufficient data.

Table 4-1. SUMMARY OF THE METEOROLOGICAL VARIABLES UNDER FOUR CATEGORIES OF CONSTRAINTS, WITH AN INDICATION OF THE CONSTRAINING VALUES

CATEGORY	VARIABLE	CONSTRAINT
1	Thunderstorm	No operation
	Rain and/or drizzle	No operation
	Freezing rain	No operation
	Snow and/or sleet	No operation
2	Ceiling/visibility	$\geq$1000 feet/3 miles
3	Headwinds	Maximum wind velocity
4	Runway density	Runway temperature < 103°F

4.2.1 Constraints Related to Hydrometeors

The variables under Category (1) are mutually exclusive in the sense that only one can be reported as "Present Weather" at a particular hour. Therefore, the percentage frequency of occurrence of the four variables in this category are simply added to form a hydrometeor group called "H" in the Venn diagrams. These data are in the form of monthly summaries for each of eight 3-hour periods per day.

4.2.2 Constraints Related to Ceiling and Visibility

The variables under Category (2) are reported jointly in the monthly summaries as the "percentage frequency of joint occurrence". The probability of C/V for "No Go" due to this constraint was similarly taken from the monthly summaries. Thus the two most important parameters, ceiling and visibility, are conveniently combined in the available statistics. They are indicated as C/V in the Venn diagrams.

4.2.3 Constraints Related to Inflight Headwinds

The variable under Category (3) is taken into account by the use of equivalent headwind data supplied by the National Climatic Center, NOAA, Asheville, N. C. These data give the mean and standard deviation of the equivalent headwind for each of the six legs (Figure 1) and for each month. The 300-mb, 500-mb, and 700-mb levels are provided.

To arrive at a transition probability for headwinds, a flight altitude of 3000 meters was selected for all legs except the westernmost leg between Edwards AFB and Tuscon. The latter segment was evaluated at 4600 meters. The specified constraints at these two levels are 9 meters per second and 14 meters per second, respectively. For eastbound flights, a map inspection of several years' upper air charts showed that the probability of encountering headwinds greater than these magnitudes is negligible in all seasons. For westbound flights, a Gaussian distribution of equivalent headwind values for the given mean and variance is assumed, and the transition probability was calculated from standard tables. The headwinds parameter is called "W" in the Venn diagrams.

4.2.4 Constraints Related to Runway Density

The variable under Category (4) has probability values which are obtained from the percentage frequency of occurrence of temperature exceeding 100°F at the instrument shelter. This constraining value is believed to be a conservative approximation to a corresponding "No Go" condition over the runway (currently assumed to be a runway temperature exceeding 103°F (see Table 4-1)). This variable is called "T" in the Venn diagrams.

4.2.5 Transition Probability Values

The transition probabilities corresponding to the four Categories are combined by the use of Eq. 16 (assuming terms beyond the second to be negligible) and Eq. 17b, yielding a set of values for each leg, for both eastbound and westbound flights, for each of four midseasonal months (January, April, July, and October). These values, which are equivalent to $T_{i,i}$, are given in Table 4-2. For example, the value .047 which appears opposite 1000 hours under leg A is the probability of "No Go" in the morning from Edwards AFB to Tuscon in January.

4.3 INCLUSION OF PERSISTENCE EFFECTS

The principal causes of delay due to persistence are found in (1) the winds at cruising levels and (2) quasi-stationary or slowly moving systems breeding inclement operational weather over route segments and terminals. The first effect influences westbound flights because easterly winds are negligible; the second effect retards eastbound flights more than westbound flights because the motion of the synoptic systems are basically eastward and a flight usually cannot penetrate the system as it moves along its flight path. The essential information for counting consecutive days of delay, or "runs", was gleaned from an examination of eight years of Daily Weather Maps of the ESSA and NOAA organizations [5,6] subsequent to 1964. These Maps contain the surface and 500-mb charts, and prior to 1969 they include a second surface map spaced 12 hours from the main chart.

4.3.1 Inflight Headwind Persistence

Headwind persistence was evaluated by noting the runs in which the opposing component of the wind at 500 mb was 40 kt or more. It is believed that this wind intensity at 500 mb usually indicates marginal conditions at lower cruising levels when the assigned constraints are observed. Three sectors consisting of two legs apiece were set up for the counting process. The result for each midseasonal month is given in Table 4-3.

Table 4-2. TRANSITION PROBABILITIES, $T_{i,i}$ FOR EACH LEG OF EASTBOUND AND WESTBOUND FLIGHTS IN EACH OF FOUR MIDSEASONAL MONTHS. THE EASTBOUND LEGS ARE DESIGNATED BY A (EDWARDS/TUSCON), B (TUSCON/EL PASO), C (EL PASO/ABILENE), D (ABILENE/SHREVEPORT), E (SHREVEPORT/EGLIN), AND F (EGLIN/KSC). THE WESTBOUND LEGS ARE DESIGNATED BY A (KSC/EGLIN), ... F (TUSCON/EDWARDS). THE FLIGHT DEPARTURE TIMES ARE 1000 AND 1300 LOCAL TIME

EASTBOUND							
JANUARY							
	A	B	C	D	E	F	
	$T_{1,1}$	$T_{2,2}$	$T_{3,3}$	$T_{4,4}$	$T_{5,5}$	$T_{6,6}$	$T_{7,7}$
1000	.047	.051	.193	.334	.334	.233	1
1300	.043	.054	.151	.493	.253	.185	1
APRIL							
1000	.015	.025	.120	.165	.160	.134	1
1300	.030	.041	.098	.115	.140	.134	1
JULY							
1000	.002	.018	.053	.067	.160	.160	1
1300	.491	.448	.167	.226	.276	.239	1
OCTOBER							
1000	.019	.022	.131	.125	.125	.103	1
1300	.036	.035	.089	.084	.017	.099	1
WESTBOUND							
JANUARY							
	A	B	C	D	E	F	
	$T_{1,1}$	$T_{2,2}$	$T_{3,3}$	$T_{4,4}$	$T_{5,5}$	$T_{6,6}$	$T_{7,7}$
1000	.631	.702	.724	.645	.456	.243	1
1300	.610	.676	.702	.629	.435	.240	1
APRIL							
1000	.491	.542	.607	.530	.358	.157	1
1300	.491	.528	.546	.519	.367	.169	1
JULY							
1000	.220	.238	.150	.297	.064	.014	1
1300	.290	.305	.198	.242	.205	.421	1
OCTOBER							
1000	.319	.332	.363	.363	.202	.069	1
1300	.306	.313	.334	.332	.208	.085	1

Table 4-3. NUMBER OF RUNS OF OCCURRENCES OF FLIGHT DELAYS DUE TO PERSISTENT HEADWINDS, FOR WESTBOUND TRIPS IN JANUARY, APRIL, AND OCTOBER. THE SECTORS ARE KSC/SHR (KENNEDY SPACEFLIGHT CENTER/SHREVEPORT), SHR/ELP (SHREVEPORT/EL PASO), AND ELP/EDW (EL PASO/EDWARDS AFB). THE DATA ARE TAKEN FROM THE DAILY WEATHER MAP(s) SERIES

			RUNS (DAYS)										
	N (Years)	SECTOR	2	3	4	5	6	7	8	9	10	11	12
January	7 1/2	KSC/SHR	4	4	3	3	2		2			1	2
		SHR/ELP	8	3	2	1	1		1	3	1		
		ELP/EDW	8	4	3					1			
April	8	KSC/SHR	4	2	1	1	1			1			
		SHR/ELP	6	3	2	2	3		2			2	
		ELP/EDW	11	5		1	2	2					
October	9	KSC/SHR	2										
		SHR/ELP	2	1	1								
		ELP/EDW	3	4	1								

The presence of persistence in these data can be investigated by a method described by Brooks and Carruthers [7, pp. 309-313]. If there is no persistence, a theoretical distribution of runs of occurrences is computed by successive evaluations of the quantity Np^kq, $k = 1, 2, \ldots n$, where N is the number of days in the sample; p is the independent probability of a constraining headwind, and is obtained as discussed in subsection 4.2.3; $q = 1 - p$; k is the number of days in the run. Thus the expected number of runs of at least 1 day, 2 days, ... n days are found. Taking the difference of adjacent values then gives the expected number of runs of exactly 1 day, 2 days, ... n-1 days.

Applying this technique to the January headwind runs, which have a value of $p = 0.555$, the theoretical and empirical frequency distributions are computed and are presented in Table 4-4, just for the KSC/SHR sector.

Table 4-4. THEORETICAL AND EMPIRICAL FREQUENCY DISTRIBUTIONS FOR THE KSC/SHR (KENNEDY SPACEFLIGHT CENTER/SHREVEPORT) SECTOR IN JANUARY. N = 232 DAYS AND p = 0.555

Calculated Value	k	2	3	4	5	6	7	8	9	10	11	12
k or more days	Np^kq	57	32	18	10	5	3	2	1	1		
k days	$\Delta(Np^kq)$	25	14	8	5	2	1	1				
Observed value												
k or more days		21	17	13	10	7	5	5	3	3	3	2
k days		4	4	3	3	2		2			1	2

The higher frequency in the last row of values, compared to the first row, when $k \geq 6$ indicates that persistence is present in the data. The next step is to assume that the probability of unfavorable conditions depends on the previous conditions. Let this probability be designated as $P(U_t/U_{t-1})$; this is the probability of not reaching the next airport, given that headwind conditions prevented flight progress on the previous trial.

Following Reference 7, the probability of 2 or more unfavorable days is given by P_{2t}. Then 3 or more unfavorable days is given by $(P_{2t})\ P(U_t/U_{t-1})$, and 4 or more by $(P_{2t})\ P^2(U_t/U_{t-1})$. Summing, this gives

$$S = P_{2t}[1 + P(U_t/U_{t-1}) + P^2(U_t/U_{t-1}) + \ldots] = \frac{P_{2t}}{1 - P(U_2/U_1)} \qquad (24)$$

which can be rewritten, where P_{2t} and S are obtained from the observed values (Table 4-4), as

$$P(U_t/U_{t-1}) = \frac{NP_{2t}}{NS} = 1 - \frac{21}{(21 + 17 + 13 + \ldots + 2)} = 0.764 \qquad (25)$$

Again, following Reference 7, a set of theoretical frequencies can be computed using $P(U_t/U_{t-1}) = 0.764$. The frequency of k or more unfavorable days is given by $N(P_{2t})P^{k-2}\ (U_t/U_{t-1})$, where NP_{2t} in Table 4-5 is 21. The differences between the values on the top line of Table 4-5 give the expected number of runs of k unfavorable days. These values are compared to the observed values of runs of k unfavorable days as given in Table 4-4.

Table 4-5. THEORETICAL AND EMPIRICAL FREQUENCY DISTRIBUTIONS FOR THE SAME SECTOR AND MONTH AS IN TABLE 4-4, BUT WITH $P(U_t/U_{t-1}) = 0.764$

Calculated Value		2	3	4	5	6	7	8	9	10	11	12
k or more days	$((21)p^{k-2}(U_t/U_{t-1})$	21	16	12	9	7	5	4	3	2	2	1
k days	$\therefore((21)p^{k-2}(U_t/U_{t-1}))$	5	4	3	2	2	1	1	1	0	1	
Observed value												
k days		4	4	3	3	2	0	2	0	0	1	

The encouraging outcome of this trial over the KSC/SHR sector led to the adoption of the above procedure to compute $P(U_t/U_{t-1})$ for each of the three sectors for January, April, and October data. The results are listed in Table 4-6.

Table 4-6. VALUES OF $P(U_t/U_{t-1})$ COMPARED WITH VALUES OF P(U) FOR THREE WESTBOUND SECTORS IN JANUARY, APRIL, AND OCTOBER. THE SECTORS ARE AS DESIGNATED IN TABLE 4-3.

MONTH	SECTOR	$P(U_t/U_{t-1})$	P(U)
January	KSC/SHR	0.764	0.555
	SHR/ELP	0.710	0.592
	ELP/EDW	0.515	0.316
April	KSC/SHR	0.643	0.435
	SHR/ELP	0.733	0.480
	ELP/EDW	0.553	0.243
October	KSC/SHR	-----	0.246
	SHR/ELP	0.428	0.270
	ELP/EDW	0.428	0.128

When the effect of headwind persistence is taken into account by Eqs. (21-23) and the data in Table 4-6, a new transition matrix is produced. This matrix includes the probabilities related to the other constraints (see Figure 3) and the newly derived headwind probabilities, which exceed the old headwind probabilities in sectors where persistence is effective. The resulting time distribution of days required for a complete trip has been evaluated by the Markov two-state chain technique. The results are presented in Section V.

4.3.2 Hydrometeor Persistence

The second effect of persistence has been analyzed by scanning the surface charts during the period when two charts per day were published in the Daily Weather Map series. The most common type of weather delay phenomenon is found to be a frontal wave in the Gulf of Mexico, with slow-moving cold fronts also accounting for a number of delay cases. Considering just eastbound flights, which suffer more delays then westbound flights, the number of cases attributable to persistent synoptic-scale phenomena has been categorized according to length of delay for the entire trip. The data do not justify a sector by sector analysis, as was done for headwinds. The results, which are quite subjective, are presented in Table 4-7.

Table 4-7. SUMMARY OF THE EFFECTS OF PERSISTENT WEATHER DELAYS ON EASTBOUND FLIGHTS IN JANUARY, APRIL, AND OCTOBER. N IS THE NUMBER OF DAYS INCLUDED IN THE SURVEY

	N (Days)	TOTAL DELAY (Days)	NO. CASES	NO. CASES/N
January	140	1 1/2	4	.029
		2	1	.007
		2 1/2	1	.007
		3	3	.022
		3 1/2	2	.014
April	104	1 1/2	1	.009
		2	1	.009
		2 1/2	2	.019
October	129	1 1/2	1	.008
		2	1	.008
		2 1/2	1	.008

The month of January is the only month studied which accrues an appreciable number of persistent weather interruptions of schedule. The probability of occurrence of an independent delay of t days was defined in subsection 2.3 (Eq. 11). In Table 4-7, the values of p_d are (see righthand column) $p_2 = .029 + .007 = .036$, $p_3 = .007 + .022 = .029$, $p_4 = .014$. Since no transition probabilities are calculable for this particular kind of delay, the results are deferred to subsection 5.3.

Section V

RESULTS

Using the procedures which have been outlined in Sections II to IV, a number of computations have been carried out for the designated Shuttle Orbiter Ferry Route in compliance with certain environmental constraints. The results of these computations are presented in the following order:

1. Cumulative time distributions of flight duration obtained by the Markov chain method, omitting persistence effects.
2. Time distributions of flight duration obtained by the Monte Carlo process, omitting persistence effects.
3. Same as 1, with persistence of inflight headwinds included.
4. Time distribution of flight duration in January based upon a survey of meteorological charts, including persistence effects of hydrometeors.
5. Sensitivity studies of the variation of constraints for inflight headwinds and ceiling/visibility, using the Markov chain technique without persistence effects.
6. Sensitivity study of an assumed interdependence among the hydrometeors, ceiling, and visibility, using the Markov chain technique without persistence effects.

5.1 MARKOV CHAIN CUMULATIVE TIME DISTRIBUTIONS

The Markov chain procedure applied under the designated constraints discussed in Section IV, and confined to takeoff times of 1000 and 1300 local time with no persistence effects operating, yields the cumulative time distributions of flight duration between Edwards AFB and KSC shown in Figure 4. This outcome is also the probability of reaching the final terminal on or before a given day. For example, in Figure 4a the July curve indicates that 87 percent of the flights in this month should traverse the eastbound route from Edwards AFB to KSC in 4 days or less. Alternatively, there is an 87-percent probability that a particular eastbound trip will complete its flight in 4 days or less. The principal difference between eastbound and westbound results, as well as the difference between the seasons, is accounted for by the headwinds factor. The greater duration of July flights eastbound, compared to the transition seasons, is caused by the occurrence of precipitation forms and high summer temperatures (in the Southwest).

5.4 ADDITIONAL INDEPENDENT DE[illegible]

The application of Eq. (1[illegible] the data of subsection 4.2 and the additional independent delays, or p_d - valu[illegible] of subsection 4.3.3, yields a new time distribution of trip duration for east[illegible]nd flights in January. The January probabilities are plotted (Figure 5a) to sh[illegible] elongation of the tail of the distribution [illegible]t the expense of shorter tri[illegible]ations of 3, 4, and 5 days. The resulting cumulative time distrib[illegible] also plotted (Figure 4a) to disclose an increase of [illegible] day [illegible] the [illegible]ent probability level of trip duration. This increase is attri[illegible] the effects of persistently inclement weather.

Such delays are minimal in other midseasonal months (Table 4-7) and they are appreciably less on westbound flights than eastbound trips. Therefore, they are not represented additionally in graphs or tables.

5.5 SENSITIVITY STUDIES

A number of computer runs were made to observe the outcome when certain Shuttle Orbiter Ferry requirements were eliminated or modified. First, the inflight headwinds constraint was studied with the other constraints held at their nominal values. Second, the ceiling/visibility constraint was studied with the other constraints eliminated.

5.5.1 Inflight Headwinds

The results of a step by step relaxation of the designated headwind constraint is related here, the limiting headwind values of 9 m sec^{-1} at ,000 m and 14 m sec^{-1} at 4000 m being multiplied by factors of 1.25, 1.50, 1.75, and 2.00. When the four midseasonal months are combined, the resulting set of cumulative percentage frequency curves show a marked improvement as the limitation is relaxed progressively (Figure 8). For example, curve "a" corresponding to the designated nominal maximum headwind indicates that 95 percent of all westbound trips traverse the KSC/Edwards AFB route in 10 days or less. However, if the headwind constraint is relaxed to twice its designated value, the result (seen in curve "e") indicates that 95 percent of all westbound trips traverse the route in 6 days or less. The conclusion reached by this sensitivity study is that the longer durations of westbound trips in winter and transition seasons can be reduced significantly if greater headwind strengths can be tolerated.

The alternative mode of presentation of Markov chain results (Figure 9) shows just the number of days required for 95 percent completion of flights. In January, 12 1/2 days are needed for 95 percent of the flights to travel this route westbound under the nominal headwind constraint. Only 7 days are needed in the latter case if the headwind constraint is relaxed to twice the designated value.

5.5.2 Ceiling Visibility

A second experiment tests the sensitivity of the most important weather-related variables, namely, the ceiling and visibility parameters, when other constraints are nil. The designated landing and takeoff minima are 1000 ft/3 mi (Category "c"). If these limits are relaxed to 500 ft/1 mi (Category "d"), the time distribution can be computed as before for comparison (Figure 10). Two other sets of limits are added for a sensitivity check at the 95-percent level.

When Categories "c" and "d" are compared, the midseasonal months of January, April, and October show a gain of about 1/2 day while July has almost no gain. A tightening of constraints to 2000 ft/5 mi (Category "b") yields a loss of nearly one day in January and a loss of about 1/2 day in the other months. A further tightening of constraints to 3000 ft/6 miles (Category "a") results in an additional extension of merely 1/2 day to one day in each month. This test therefore reveals little sensitivity in the ceiling and visibility, in comparison with the headwind constraint.

5.6 INTERRELATIONSHIPS AMONG HYDROMETEORS, CEILING, AND VISIBILITY

Although the above results assume that the events (e.g., the meteorological record of constraining factors) are independent, but not mutually exclusive, this assumption is not strictly defensible. The degree of correlation between the various factors is not known. However, some interdependence can be expected between the hydrometeors and the ceiling/visibility parameter. A very optimistic assumption would be to state that such events are inclusive in the sense that the greatest probability of occurrence within Categories 1 and 2 (Table 4-1) represents that pair of Categories. When this substitution is made, the new set of transition probabilities gives a more optimistic result which may be regarded as a lower bound on the number of days required for a complete trip in each season. The outcome for eastbound and westbound trips, using the nominal headwind limits specified for the problem, is entered in Figure 7. Thus, in January the optimistic limit for eastbound flights is 4 1/2 days, compared to 5 days for the nominal case, whereas this limiting value for westbound flights is 11 1/2 days, compared to 12 1/2 days for nominal ceiling and visibility constraints. Thus, the reduction of trip duration attributable to interdependence among hydrometeors, ceiling, and visibility is rather minimal.

Section VI

CONCLUSIONS

The Markov chain and Monte Carlo analyses are effective methods to determine probable flight times for Space Shuttle ferrying operations. Furthermore, the techniques used in this study are applicable to other routes and other transport configurations.

Because of the assumption that only one leg can be completed each half-day, the present results indicate that the designated Shuttle Orbiter route and requirements correspond to an absolute minimum period of 3 days. This period is needed to traverse the six-leg path between Edwards AFB and Kennedy Spaceflight Center, flying in either direction.

Eastbound flights are found to be free of ground delays caused by the designated headwind constraint of 9 m sec^{-1} at 3000 m and 14 m sec^{-1} at 4600 m. However, the other constraints (e.g., ceiling, visibility, and hydrometeors) result in a 95-percent probability of completion within 5 days in any season. Conversely, there is a 5-percent risk of exceeding 5 days in a flight started at random. Persistently unfavorable weather conditions extend the expected delay period an additional day in winter.

Westbound flights are affected by the designated headwind constraint in winter and in transition seasons. Evaluation of the ground delays caused by this factor and the other constraints reveal an annual 95-percent completion level ranging from 5 days in July to 13 days in January. Inclusion of persistence in the headwinds has little effect except in winter, when the 13-day figure is raised to 17 days.

Sensitivity tests upon the headwind constraint indicate that relaxation of this factor significantly reduces the 95-percent probability time. For example, increasing the limit to 1 1/2 times its designated value reduces the 13-day figure to 9 days. On the other hand, the adjustment of ceiling/visibility constraints has little effect upon flight duration.

Section VII

REFERENCES

1. Brodie, S. B., "Saturn V Launch Vehicle and Spacecraft Launch Probability", Lockheed Missiles and Space Company, Final Report, April 1969.
2. Shreider, Yu, A., "The Monte Carlo Method", Pergamon Press, 1966.
3. Cohen, A Clifford, "Probabilities of Sequences of Favorable and Unfavorable Launching Intervals", Technical Report Number 27, The University of Georgia, 1968.
4. Revised Uniform Summary of Surface Weather Observations, Data Processing Division, ETAC/USAF, Air Weather Service (MATS), Asheville, N. C.
5. Daily Weather Map, U. S. Department of Commerce, Weather Bureau, Washington, D. C.
6. Daily Weather Maps, U. S. Department of Commerce, ESSA (NOAA) Environmental Data Service, Silver Spring, Md.
7. Brooks, C. E. P. and Carruthers, N., "Handbook of Statistical Methods in Meteorology", London, 1953, pp. 309-313.

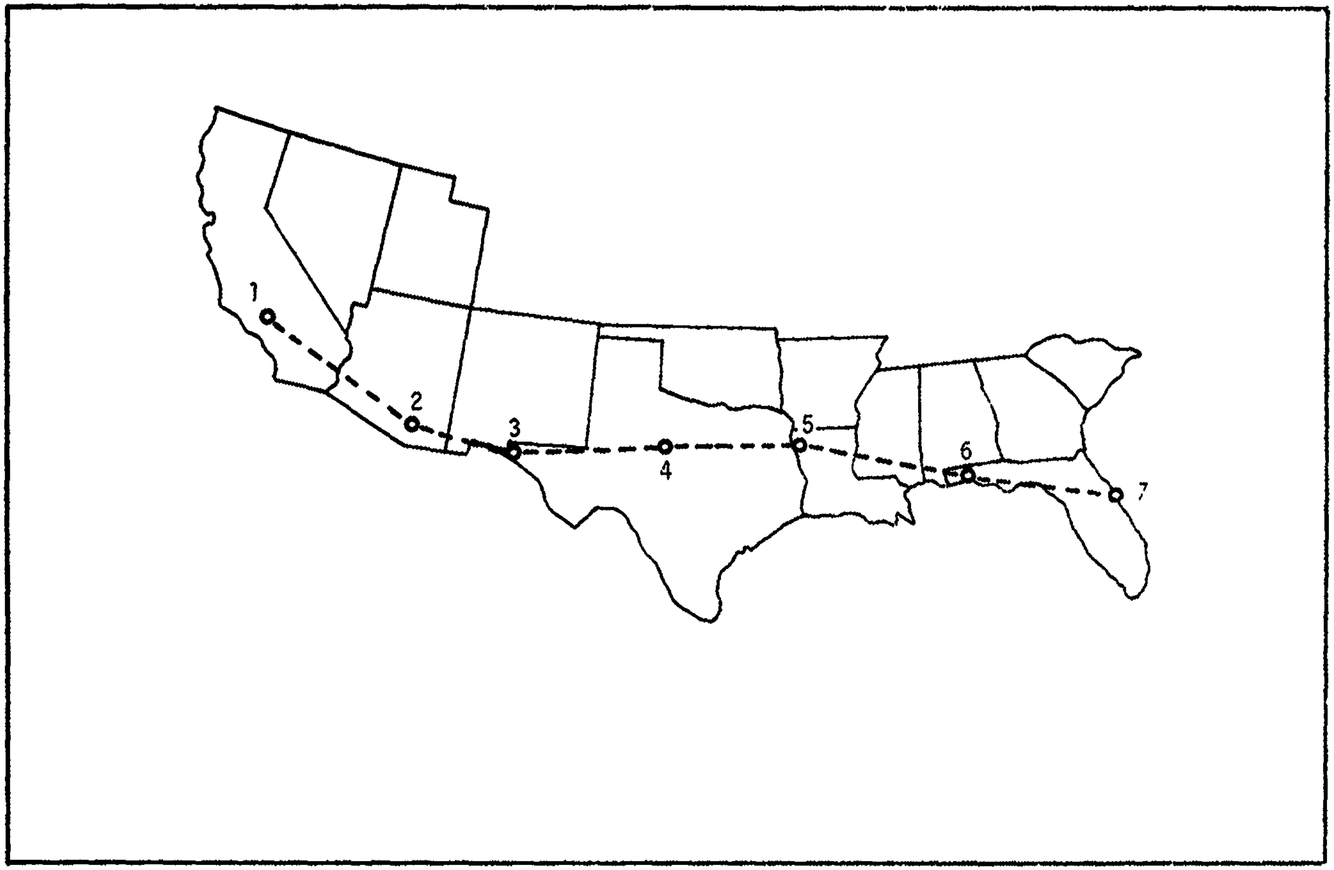

Figure 1. ROUTE OF THE SPACE SHUTTLE ORBITER FERRY VEHICLE. THE TERMINALS NUMBERED 1 TO 7 HAVE THE FOLLOWING NAMES: 1 - EDWARDS AFB, 2 - TUSCON (DAVIS-MONTHAN AFB), 3 - EL PASO (BIGGS AFB), 4 - ABILENE (DYESS AFB), 5 - SHREVEPORT (BARKSDALE AFB), 6 - EGLIN AFB, 7 - KENNEDY SPACEFLIGHT CENTER

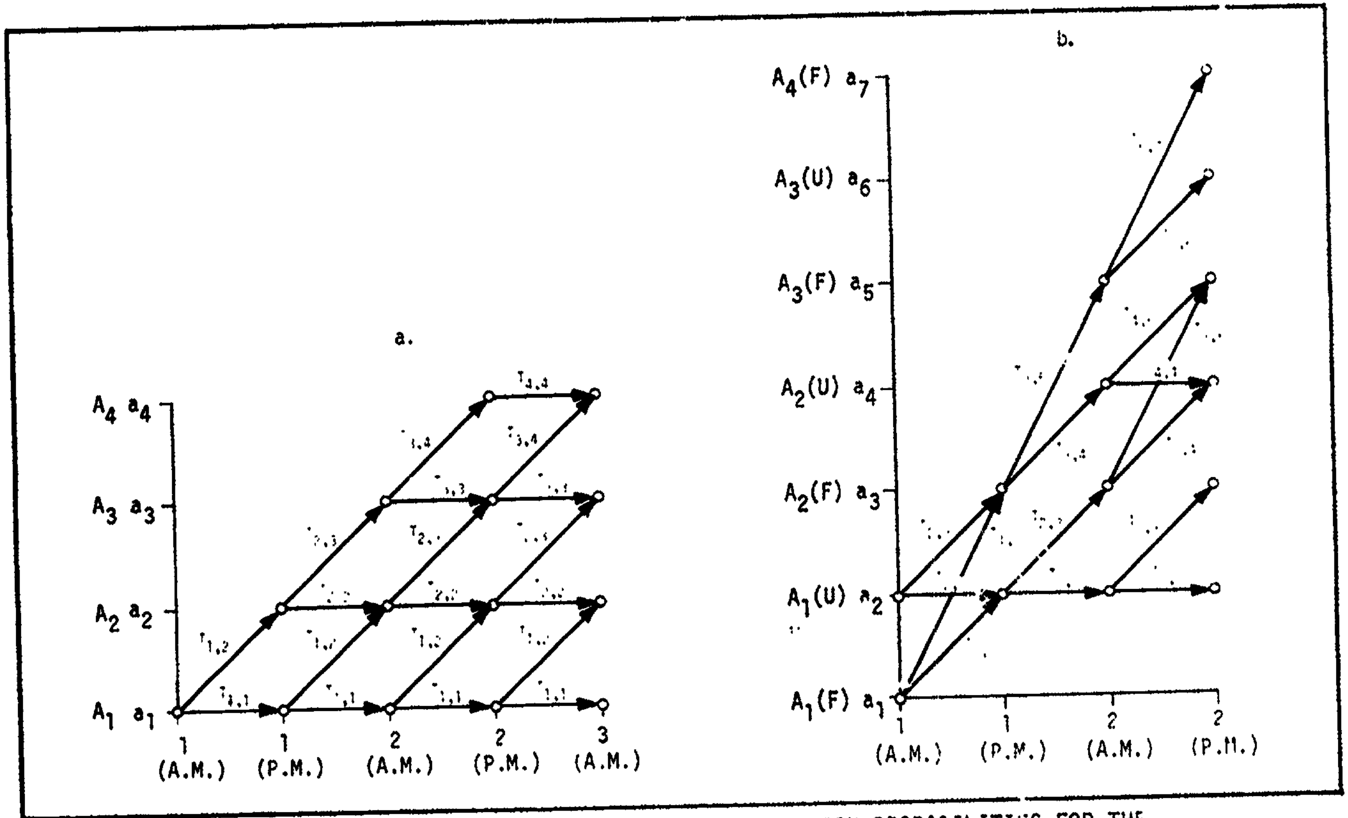

Figure 2. SCHEMATIC DIAGRAM OF STATES AND TRANSITION PROBABILITIES FOR THE CASE WITH NO PERSISTENCE IN CONSTRAINING EFFECTS (2a) AND THE CASE WITH PERSISTENCE (2b). THE A_i DESIGNATE AIRPORTS AND THE a_i REPRESENT STATES. 1 (A.M.) REPRESENTS A MORNING TRIAL THE ı .RST DAY, 2 (P.M.) AN AFTERNOON TRIAL THE SECOND DAY, ETC. U INDICATFS PREVIOUSLY UNFAVORABLE CONDITIONS, F INDICATES PREVIOUSLY FAVORABLE CONDITIONS. THE LINES SHOW VARIOUS POSSIBLE PATHS OF PROGRESS IN THE MARKOV CHAIN METHOD.

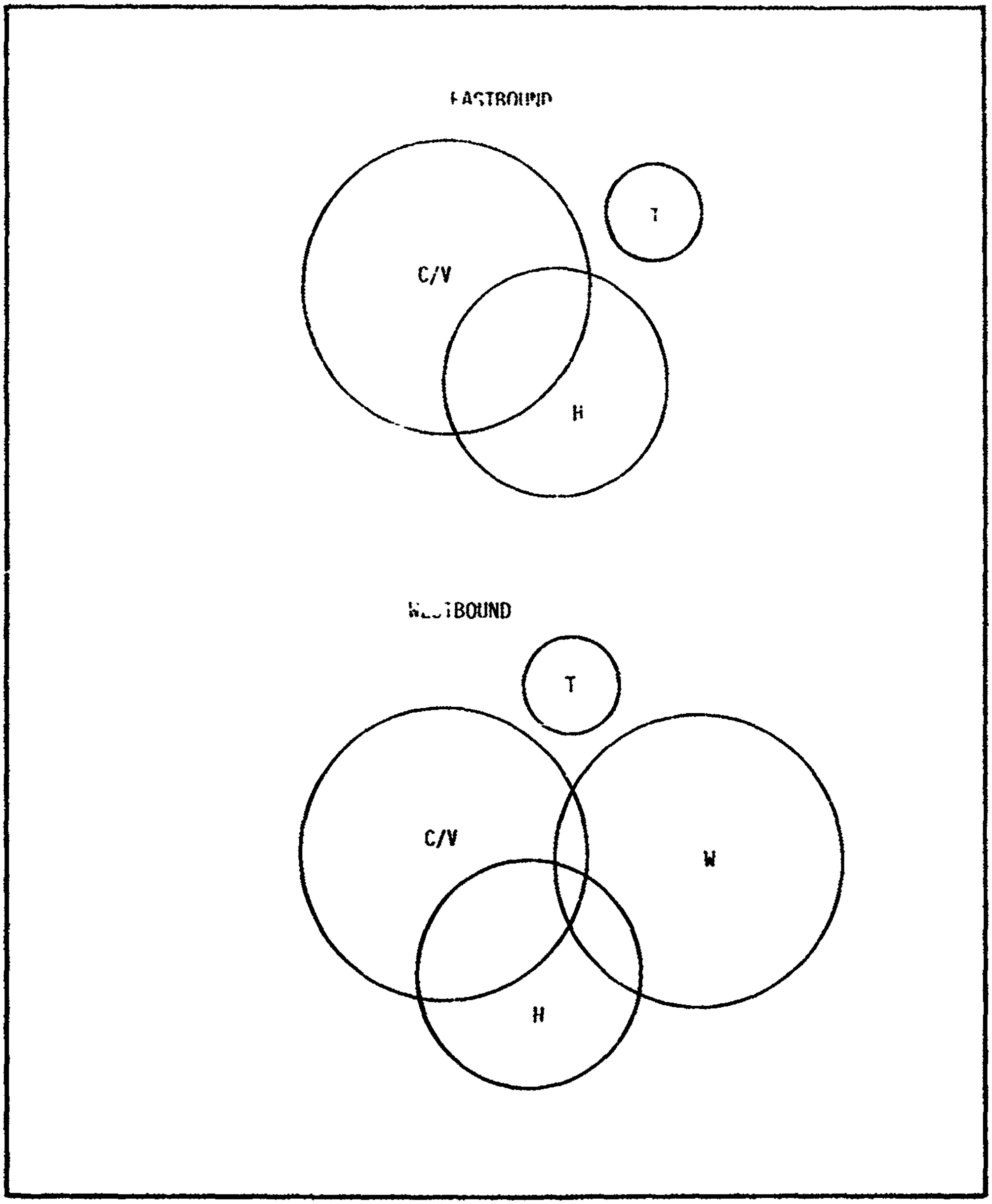

Figure 3. SCHEMATIC VENN DIAGRAM OF THE CONSTRAINING FACTORS FOR EASTBOUND AND WESTBOUND FLIGHTS, SHOWING A DEGREE OF INTERRELATIONSHIP. THE LETTER DESIGNATORS HAVE THE FOLLOWING MEANING: C/V - CEILING/VISIBILITY, H - HYDROMETEORS, T - RUNWAY TEMPERATURE, W - HEADWINDS

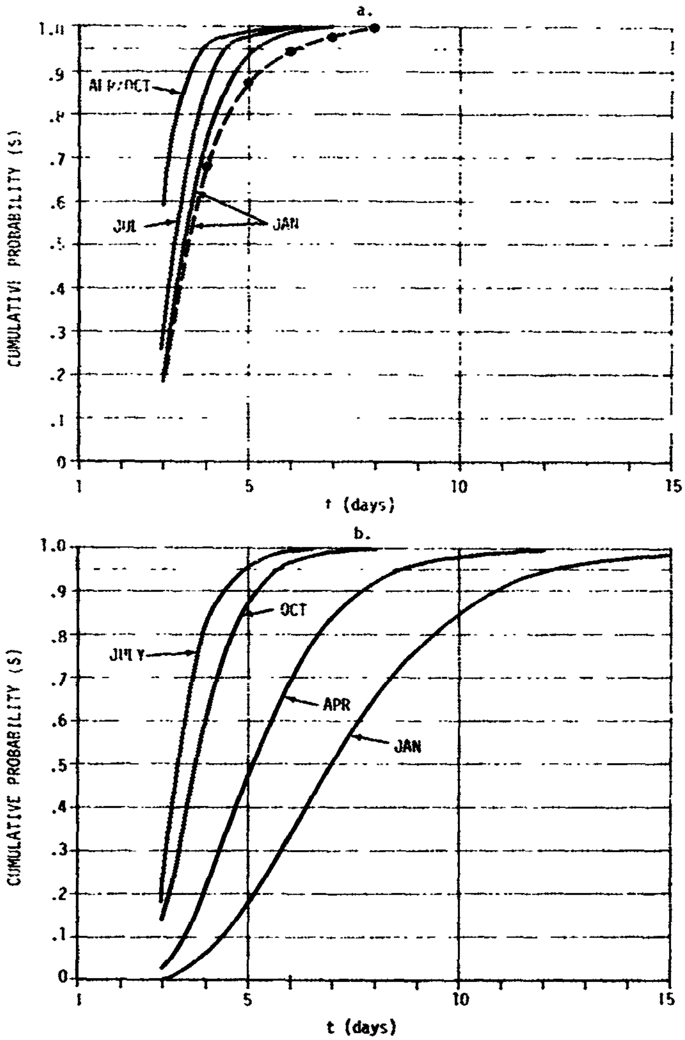

Figure 4. CURVES OF CUMULATIVE PROBABILITY FOR NUMBER OF DAYS (t) REQUIRED TO FLY BETWEEN EDWARDS AFB AND KSC, EASTBOUND (4a) AND WESTBOUND (4b), FOR JANUARY, APRIL, JULY, AND OCTOBER. THE CONSTRAINTS LISTED IN TABLE 1 ARE APPLIED, WITHOUT PERSISTENCE EFFECTS, TO OBTAIN THE CONTINUOUS CURVES. THE EFFECTS OF PERSISTENT, INCLEMENT WEATHER (SECTION V) ARE INCLUDED TO OBTAIN THE BROKEN CURVE IN 4a. THE MARKOV CHAIN PROCEDURE IS THE RELEVANT TECHNIQUE

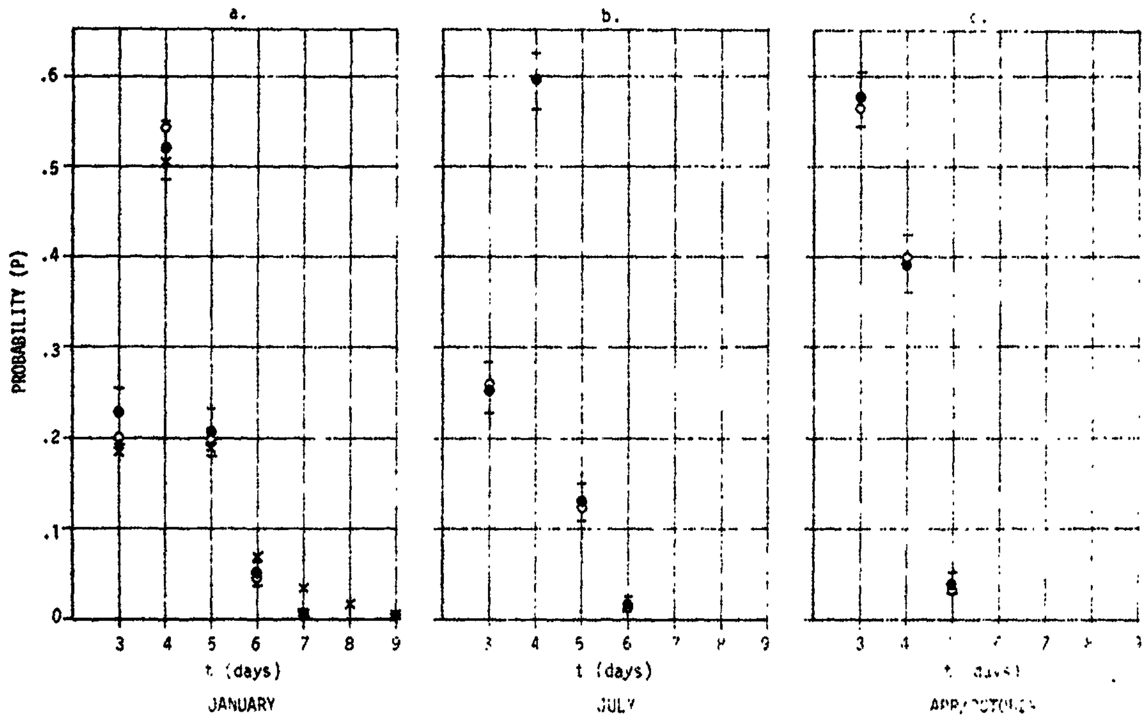

Figure 5. PROBABILITY OF THE NUMBER OF DAYS (t) REQUIRED TO FLY EASTBOUND TRIPS FROM EDWARDS AFB TO KSC IN JANUARY (5a), JULY (5b), AND APRIL/OCTOBER (5c). THE DOTS AND SHORT HORIZONTAL LINES ARE THE VALUES AND TWO-SIGMA CONFIDENCE LIMITS, RESPECTIVELY, FOR CALCULATIONS MADE BY THE MONTE CARLO METHOD. CIRCLES REPRESENT VALUES FOUND BY THE MARKOV CHAIN PROCESS. X's ARE VALUES OBTAINED WHEN THE EFFECTS OF PERSISTENTLY INCLEMENT WEATHER ARE INCLUDED

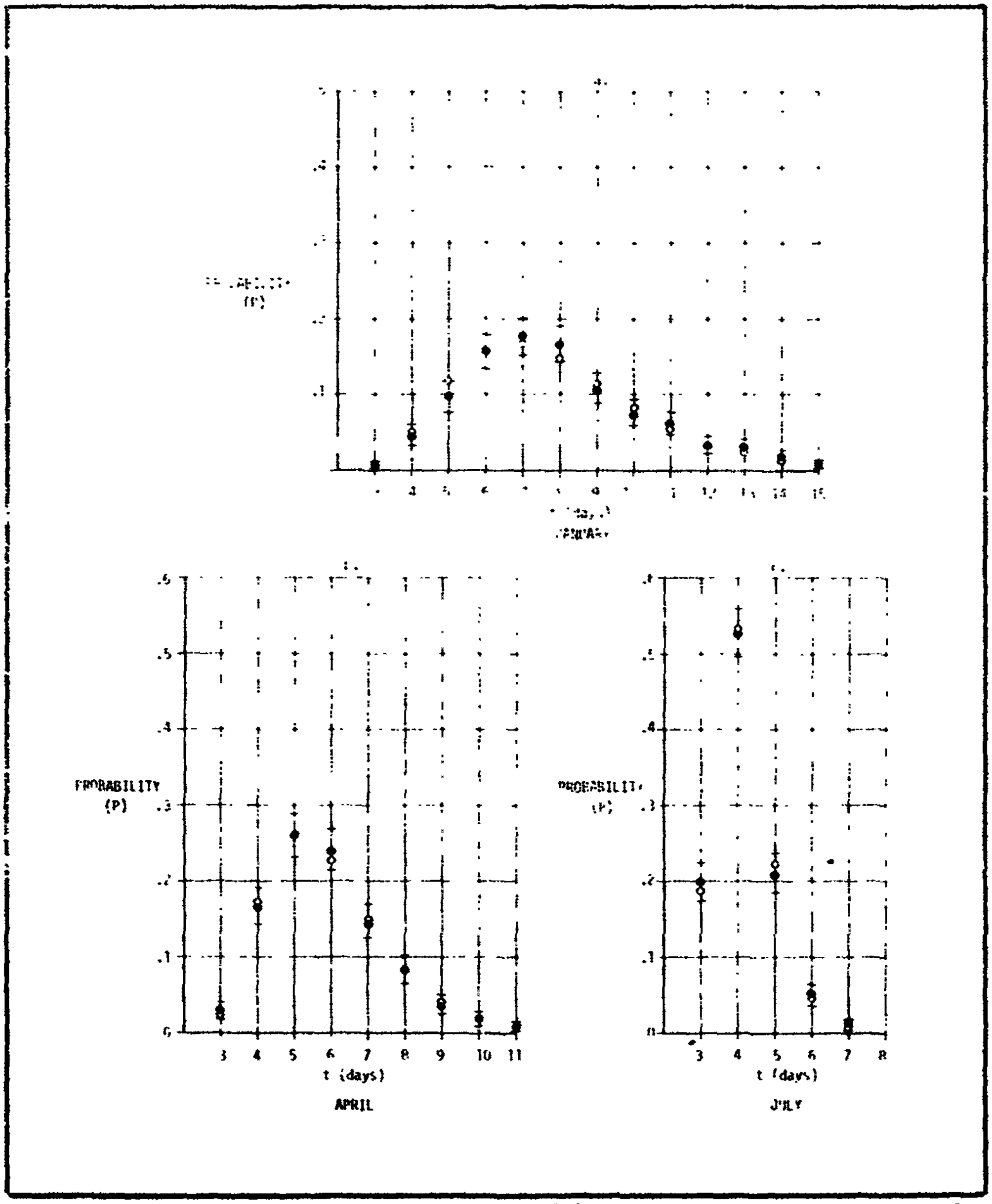

Figure 6. PROBABILITY OF THE NUMBER OF DAYS (t) REQUIRED TO FLY WESTBOUND TRIPS FROM KSC TO EDWARDS AFB IN JANUARY, (6a), APRIL (6b), AND JULY (6c). THE DOTS AND SHORT HORIZONTAL LINES ARE THE VALUES AND TWO-SIGMA CONFIDENCE LIMITS, RESPECTIVELY, FOR CALCULATIONS MADE BY THE MONTE CARLO METHOD. CIRCLES REPRESENT VALUES FOUND BY THE MARKOV CHAIN PROCESS.

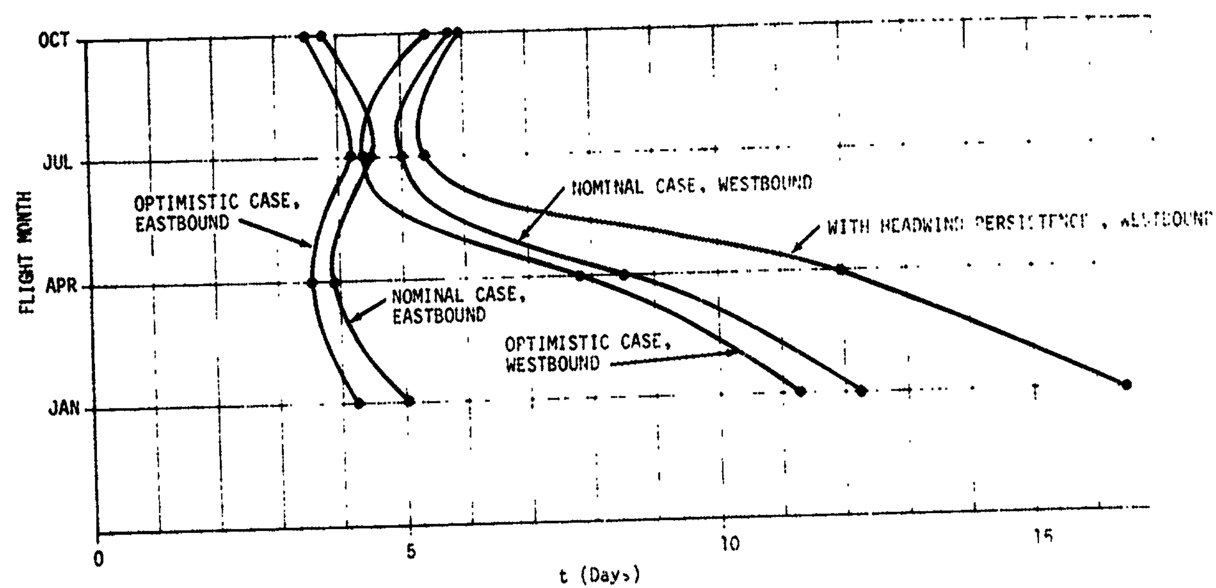

Figure 7. 95-PERCENT PROBABILITY VALUES FOR THE NUMBER OF DAYS (t) REQUIRED TO FLY EASTBOUND AND WESTBOUND TRIPS IN JANUARY, APRIL, JULY, AND OCTOBER UNDER DESIGNATED CONSTRAINTS. THE "OPTIMISTIC CASE" VALUES FOR THE SAME MONTHS ARE BASED UPON HYDROMETEOR CONSTRAINTS WHICH ARE INCLUSIVE. THE OUTCOME INCLUDING HEADWIND PERSISTENCE IS ADDED FOR WESTBOUND FLIGHTS. THE MARKOV CHAIN METHOD IS THE RELEVANT PROCEDURE

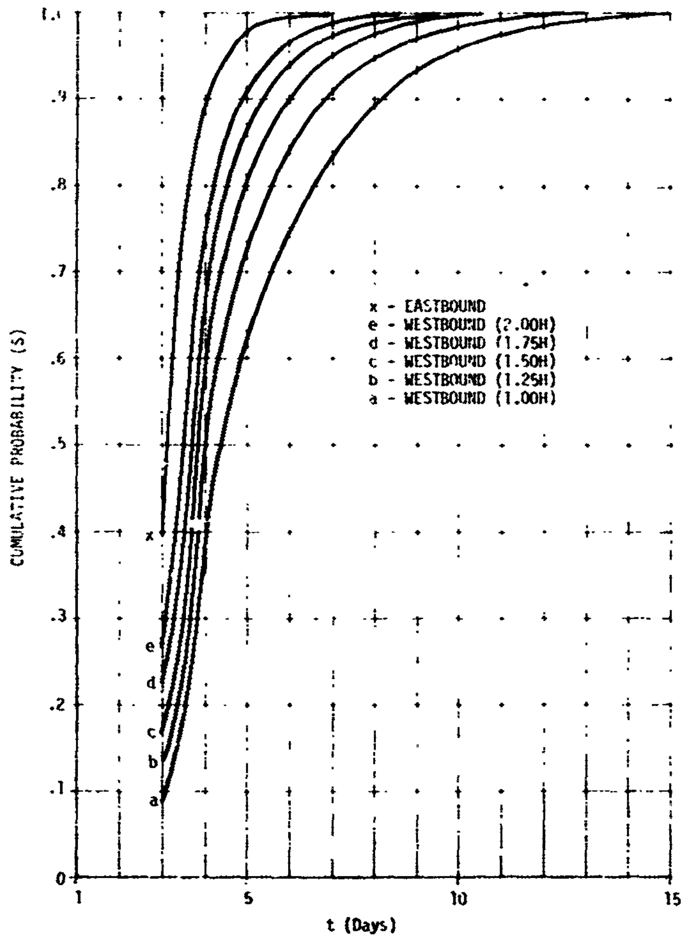

Figure 8. ANNUAL CURVES OF CUMULATIVE PROBABILITY FOR NUMBER OF DAYS (t) REQUIRED TO FLY BETWEEN EDWARDS AFB AND KSC, EASTBOUND AND WESTBOUND, FORMED BY AVERAGING THE DATA FOR JANUARY, APRIL, JULY, AND OCTOBER. CURVES a (WESTBOUND) AND X (EASTBOUND) ARE BASED UPON THE DESIGNATED HEADWIND CONSTRAINTS OF 9 m sec^{-1} AT 3.0 km AND 14 m sec^{-1} AT 4.6 km, THE TWO FLIGHT LEVELS USED IN THE COMPUTATIONS. CURVES b, c, d, AND e (ALL WESTBOUND) ARE BASED UPON A RELAXATION OF THE HEADWIND CONSTRAINT, IN STEPS OF ONE-QUARTER, TO A MAXIMUM RELAXATION OF 2.00H. H REFERS TO EITHER OF THE DESIGNATED HEADWIND CONSTRAINTS. THE MARKOV CHAIN PROCESS IS THE RELEVANT METHOD

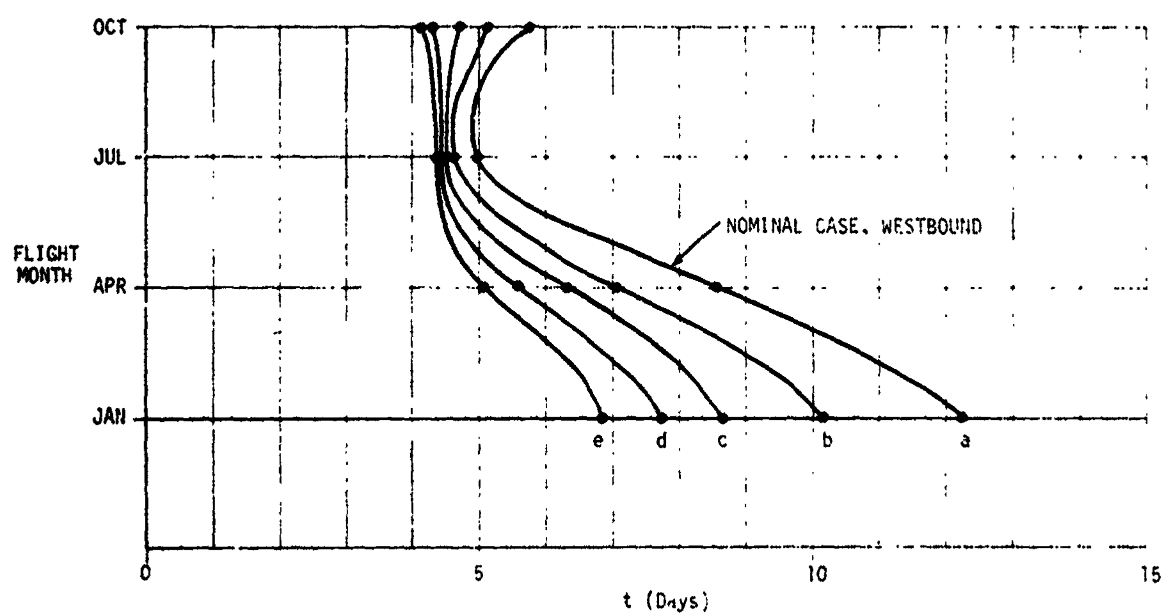

Figure 9. 95-PERCENT PROBABILITY VALUES FOR THE NUMBER OF DAYS (t) REQUIRED TO FLY WESTBOUND TRIPS IN JANUARY, APRIL, JULY, AND OCTOBER UNDER DESIGNATED CONSTRAINTS (CURVE a) AND UNDER RELAXED HEADWIND CONSTRAINTS AS IN FIGURE 8 (CURVES b, c, d, AND e). THE MARKOV CHAIN PROCESS IS THE RELEVANT METHOD

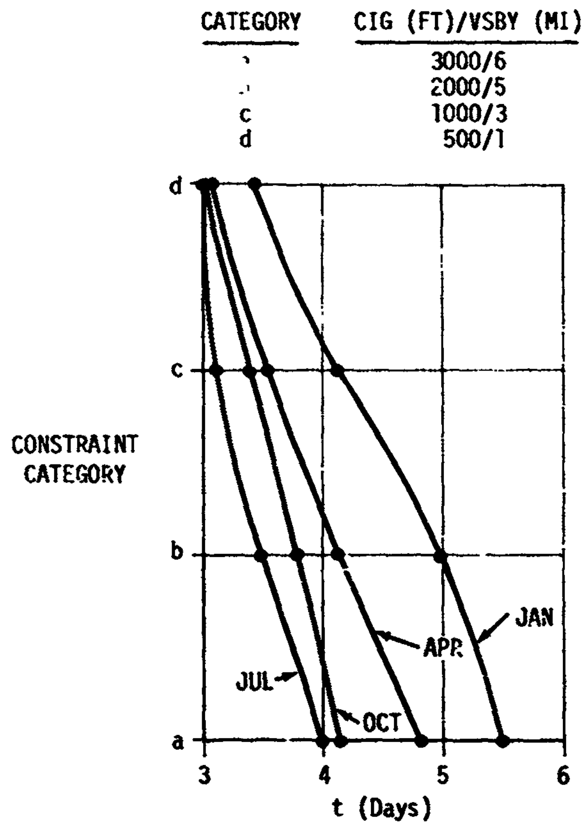

Figure 10. 95-PERCENT PROBABILITY VALUES FOR THE NUMBER OF DAYS (t) REQUIRED TO FLY EASTBOUND OR WESTBOUND TRIPS IN JANUARY, APRIL, JULY, AND OCTOBER, UNDER FOUR COMBINATIONS OF THE CEILING/VISIBILITY CONSTRAINT. THE OTHER CONSTRAINTS ARE NIL. THE MARKOV CHAIN PROCESS IS THE RELEVANT METHOD